Using LIDAR data in a quantitative appraisal of post-extreme event erosion phenomena

Example of the Baillmarsane catchment area (Escaro, Pyrénées-Orientales) following Storm Gloria in the Mediterranean

Interreg Sudoe
MONTCLIMA
European Regional Development Fund

Table of contents

1. GENERAL CONTEXT

The example described in this guide concerns the Risk Basin Study (EBR) commissioned by the Ministry of Agriculture and Food (MAA) from the Mountain Terrain Rehabilitation (RTM) department in the Pyrénées-Orientales. Drafting an EBR involves collecting as much exhaustive information as possible in order to address all aspects of the catchment area. Following exploitation of the data, the document reviews current knowledge of the protection and hazard management systems in order to set out a programme of action drawing upon baseline and hazard limitation scenarios addressing the threats identified.

The Baillmarsane catchment area (15 km²) is located in the municipalities of Escaro and Serdinya *(Figure 1)* on the northern flank of the Très Estelles massif (2,099 m). It flows into

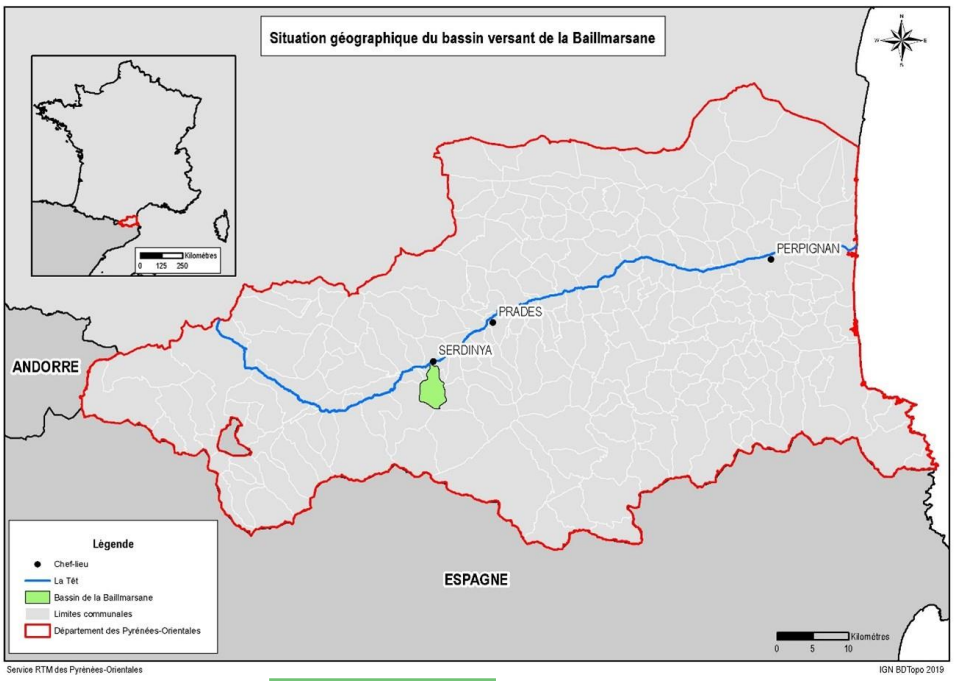

Figure 1: Map showing the geographical location of the Baillmarsane. catchment area

the Têt (540 m). Although it accounts for just 1% of the Têt catchment area, the importance of the Baillmarsane is far greater in terms of gravity-related phenomena, the deposition of materials and torrentiality.

Since the end of the 19th century and the acquisition of land by the State, a number of strategies have been implemented to reduce the frequency and intensity of a wide range of phenomena (overflowing watercourses, erosion and gullying, landslides). The objectives are multiple: to slow down torrential dynamics and the longitudinal incision rate, to drain off surface water, and to prevent erosion of the slopes. The Baillmarsane catchment area is unusual in that only the tributaries of Baillmarsane are included in the perimeter of the Conflent national forest. The hydrographic network comprises several major and secondary gullies that cut deeply into the slopes and regularly cause significant events. These gullies are where the so-called RTM structures are found *(Figure 2)*.

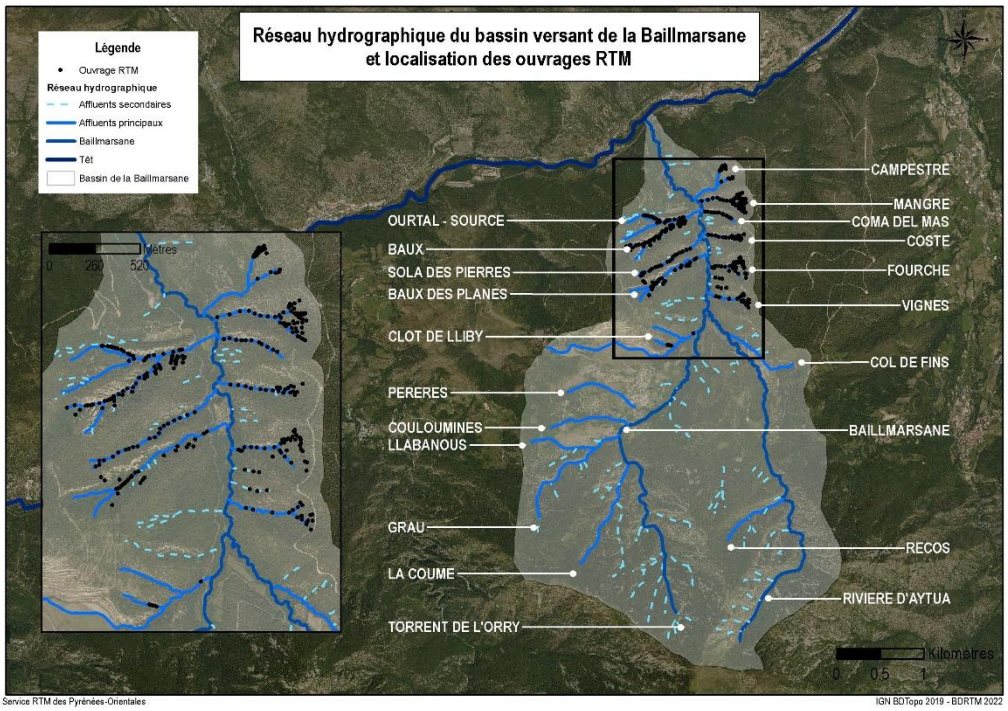

Figure 2: Map of the hydrographic network of the Baillmarsane catchment area showing the location of RTM. structures

By using and comparing LIDAR data as part of the EBR, we can quantify erosion phenomena. Putting this quantitative information into perspective is particularly useful following an extreme rainfall event. As a result of climate change, this type of event is becoming more frequent and causing increasing levels of damage. The purpose of this guide is to provide key information for using LIDAR data in a post-event situation on terrain that is vulnerable to erosion.

2. Purpose of this guide

Climate change is leading to more frequent and more extreme rainfall events, with increasingly severe consequences, particularly in relation to the phenomena discussed here. In mountain areas, it is particularly important to consider physical environmental factors (geological formations, orientation, slopes, land use, type of vegetation, etc.), which play a key role. Implemented alongside field surveys, LIDAR campaigns provide an overall view of these factors on different scales. These data enable more detailed appraisals, to understand or mitigate phenomena, or to suggest protective measures.

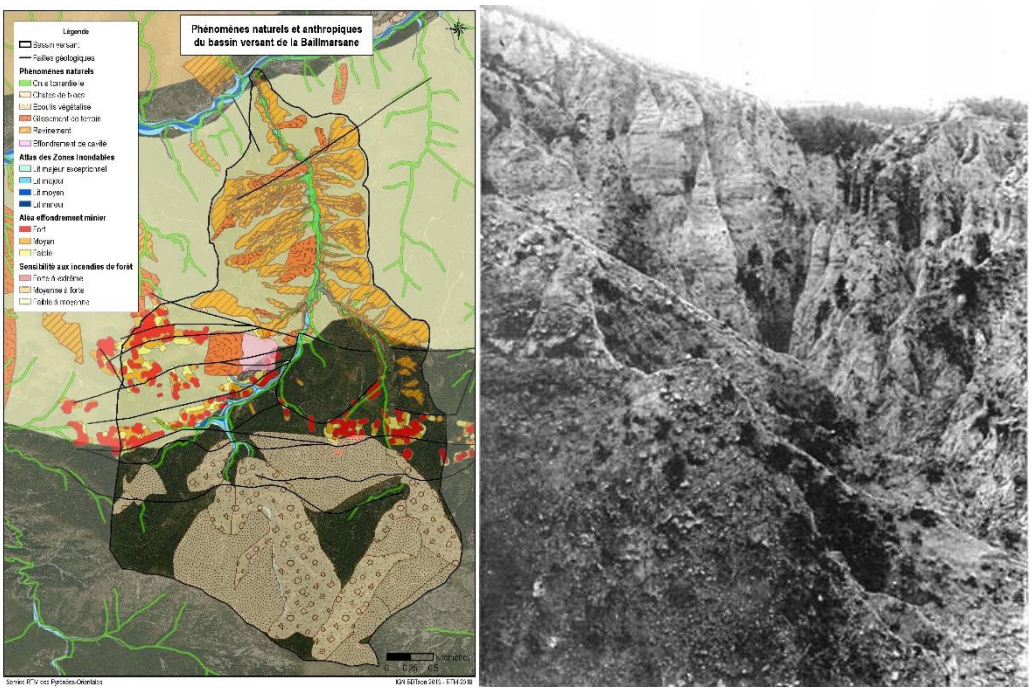

Figure 3: (left) Map of natural and anthropogenic phenomena in the Baillmarsane catchment area; (right) View of the land in the upper part of the Baux sub-catchment area at the end of the nineteenth century.

The example of the Baillmarsane catchment area provides a practical framework for the theory developed above. The EBR focuses on the lower part of the Baillmarsane, which is primarily made up of Miocene conglomeratic terrain (an alternation of coarse, unsorted quartzo-feldspathic sands with metric blocks primarily made up of gneiss). Despite a uniform geology *(Figure 5 A)*, each gully is unique. This is the result of several factors such as the stratification of this conglomeratic formation: the dip and induration of the strata play important roles at local level in the occurrence of land movements and erosion *(Figure 3)*.

The orientation of the land *(Figure 5 B)* has an impact on the physiognomy of the soil and banks as well as on the dynamics of vegetation cover. Differences can thus be observed between the slopes that are south-facing (dry and stony soil with sparse shrubby vegetation) and those that are north-facing (wetter soil with more intense vegetation dynamics). Furthermore, this terrain is located in the flattest part of the catchment area with a gradient generally lower than 30° *(Figure 5 C)*.However, owing to the lower level of rock competence, torrential incisions in this geological formation are creating gullies whose steeply sloping banks can reach gradients of over 45°, sometimes even rising vertically over several dozen metres. The erosive power of the water is considerable, creating typical badlands.

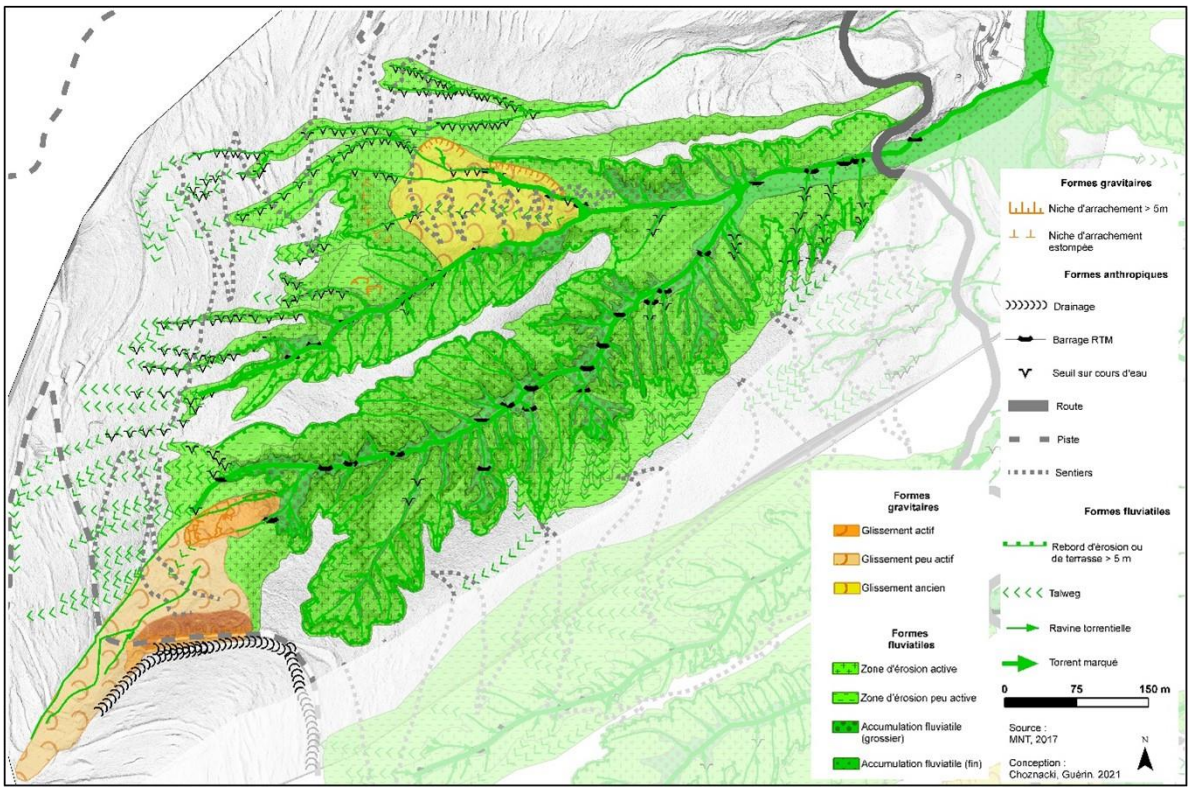

Figure 4: Geomorphological map of the Baux sub-catchment area (extract from EBR, 2022)

Today, the forest covers almost 70% of the catchment surface area, compared to just a few percent at the end of the 19th century *(Figures 3 and 5 D)*. Since the successful planting trials organised from 1889 onwards, the objective has been to maintain plant cover in order to protect this erosion-sensitive soil. Despite a high level of afforestation and, until recently, a low frequency of extreme events, the gullies react systematically and at speed in the event of high torrentiality. Finally, by conducting a geomorphological analysis of the terrain *(Figure 4)*, we are able to characterise the various sub-catchment areas, as well as to analyse the interlinking of the various phenomena and how they translate on the ground (erosion, incision, accretion, etc.).

Extreme weather events are impacting soil protection and the production of solid materials. These questions were raised in the wake of Storm Gloria in the Mediterranean. A rain and snow storm took place between 20 and 23 January 2020, when storm Gloria hit the western Mediterranean basin, moving into southern France. This storm had a severe impact on the coastline (coastal flooding with waves of between 5 and 8 m), the plains (a significant accumulation of rainfall), and the foothills and mountain areas (impacted by both liquid and solid accumulations). The equivalent of 4 to 5 months of rainfall fell in just 72 hours. These high levels of accumulation led to exceptional floods across the department *(Figure 6)*.

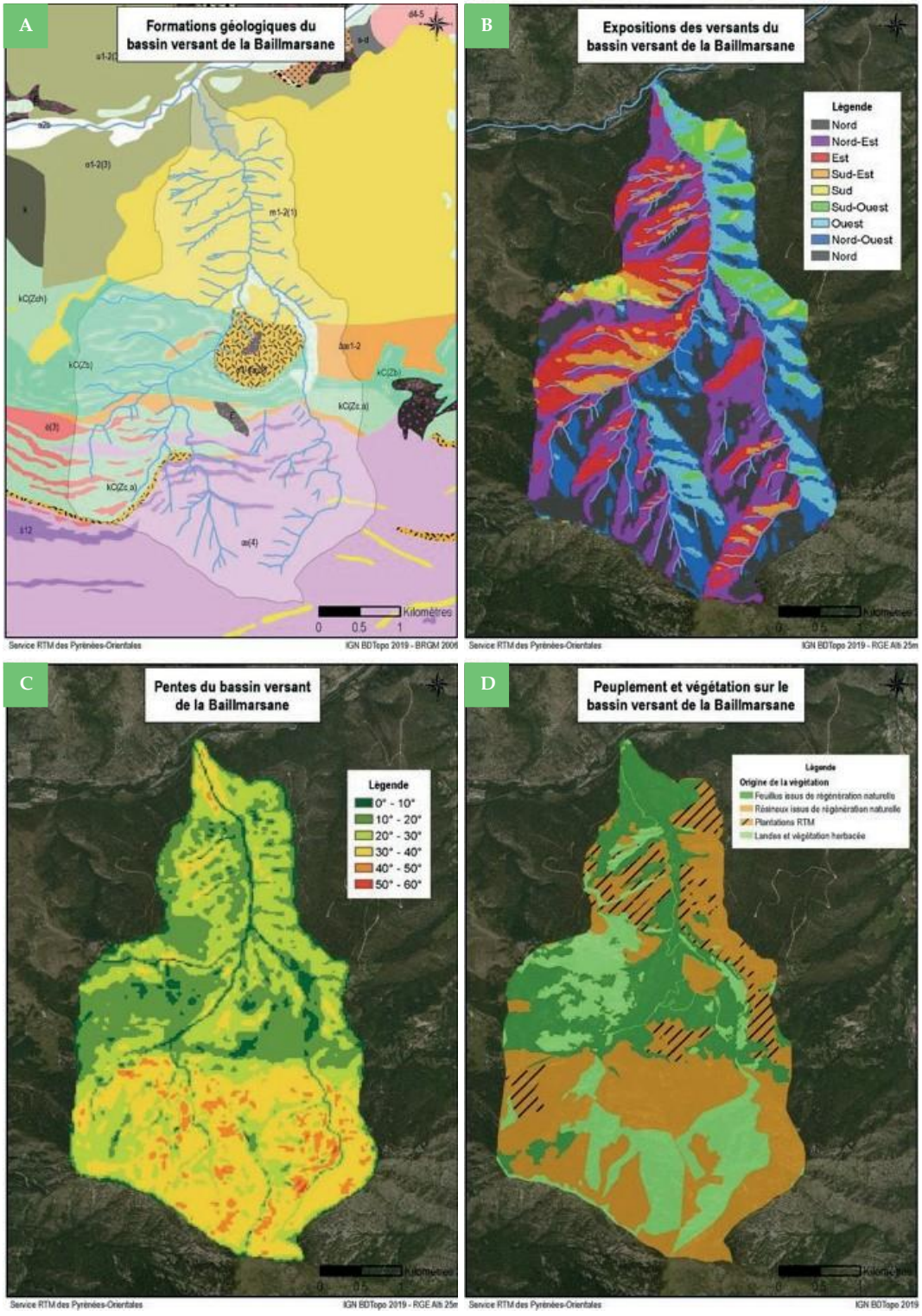

Figure 5: Maps of geological formations (A), orientation of the slopes (B and C), and vegetation (D) in the Baillmarsane. catchment area

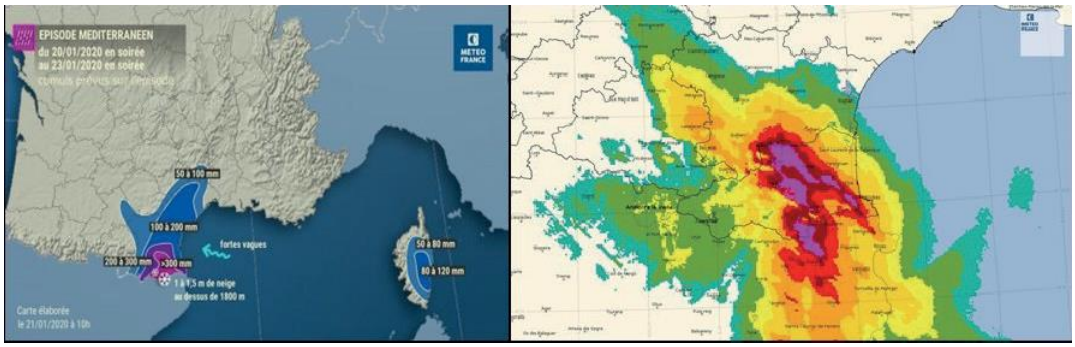

Figure 6: Météo France maps showing the storm on 21/01/2020 and the cumulative water level over 72 hrs (20/01/2020 14h to 23/01/2020 10h).

Figure 7: Views of the gully from the RD27 looking towards Escaro and a structure in the Baux ravine after storm Gloria.

Rain events of this type are fairly uncommon on the Mediterranean rim in winter. This one was unusual for the alternation of rain and snow, caused by altitudinal fluctuation of the 0°C isotherm. This alternation considerably modified the surface runoff regime, leading to significant infiltration rates, increasing soil instability. A considerable number of land movement and erosion phenomena were listed *(Figure 7)*. In addition, the DREAL report of 12 February 2020 said that the Têt experienced a ten-yearly flooding episode that was more significant than usual, over its entire course, from Mont-Louis to Perpignan, as well as on its tributaries.

In view of the intrinsic characteristics of this terrain, which is vulnerable to erosion phenomena following a major event such as Storm Gloria, the Mountain Terrain Rehabilitation department began a study to quantify erosion phenomena and the impact of an event of this magnitude by comparing pre- and post-event LIDAR data for the Baillmarsane catchment area.

3. Proposals for LIDAR data processing

Using LIDAR data enables the quantitative estimate and spatial analysis of erosion phenomena. Following a series of data processing steps, it is possible to identify zones of erosion and accretion as well as a range of volumes allowing us to establish direct links between these zones. The purpose of this guide is to provide examples of the data processing steps carried out as part of the Baillmarsane EBR, for transposition to similar surveys.

As part of the EBR, two LIDAR campaigns were carried out by the same service provider: one in 2018 in preparation for the study and the other in 2021 following the Mediterranean event. The main characteristics of the two campaigns (2018 and 2021 A) are shown below (Figure 8), alongside a final campaign (2021 B). This last operation was a repeat of the 2021 survey, organised on the request of the RTM department, in view of a significantly lower level of quality compared with the 2018 survey. The 2021 campaigns involved a homogeneous global survey over the entire area, and a high-definition survey focusing exclusively on the most problematic sub-catchment areas with an observable response to key issues during Storm Gloria.

	Commande 2018	Commande 2021 A		Commande 2021 B	
		Global	HD	Global	HD
Matériel	LIDAR Riegl avec centrale inertielle IXBLUE AIRINS III monté sur un Partenavia P68	LIDAR Riegl avec centrale inertielle IXBLUE AIRINS III, GPS Trimble et caméra IXU RS 1000 montés sur un Partenavia P68			
Date du vol	5 avril 2018 entre 8h10-12h25	8 juin 2021 entre 8h30-14h30		19 novembre 2021 entre 9h15-13h55	
Emprise sur le BV	Baillmarsane partie inférieure	Baillmarsane en totalité		Baillmarsane en totalité	
Hauteur de vol (m)	950 m	1550 m	1300 m	1370 m	1100 m
Vitesse de vol (km/h)	150 km/h	205 km/h	205 km/h	205 km/h	205 km/h
Fréquence d'émission laser (kHz)	400 kHz	1100 kHz	2000 kHz	600 kHz	1100 kHz
Largeur de bande de vol (m)	1100 m	1790 m	1500 m	1580 m	1270 m
Recouvrement latéral (%)	52%	55%	78%	70%	80%
Angle de scan	60°	60°	60°	60°	60°
Diamètre de la tâche LIDAR	24 cm	29 cm	24 cm	25 cm	20 cm
Densité (pts/m²)	11 pts/m²	14 pts/m²	45 pts/m²	13.5 pts/m²	50 pts/m²
Résolution d'acquisition (cm)	9 cm	10 cm	4 cm	-	-
Contrôle de la précision	5 relevés : écarts < 10 cm	4 relevés : écarts < 10 cm		4 relevés : écarts < 10 cm	

Figure 8: Table of the main characteristics of the various LIDAR surveys described in mission reports.

The difference in quality between the 2021 A and 2018 campaigns was raised with the service provider, based on several screenshots of areas in which the point density appeared to be insufficient (Figure 9). The more recent data received and approved showed a level of quality that was more in line with expectations, enabling post-processing operations by the RTM. department.

In order for this data processing to be carried out, pre-processing must be carried out by the service provider. This requirement must be clearly indicated in the order specifications. The first processing step involves classifying the points based on the type of object reflecting the laser pulse. This classification is standardized by the ASPRS[1]. It takes the form of a code between 0 and 18 written in files with the format .las. The specification must list the codes and their meanings. In particular, the point classification process makes it possible to produce DTMs that do not take account of points classified as vegetation, for example.

1. American Society for Photogrammetry and Remote Sensing.

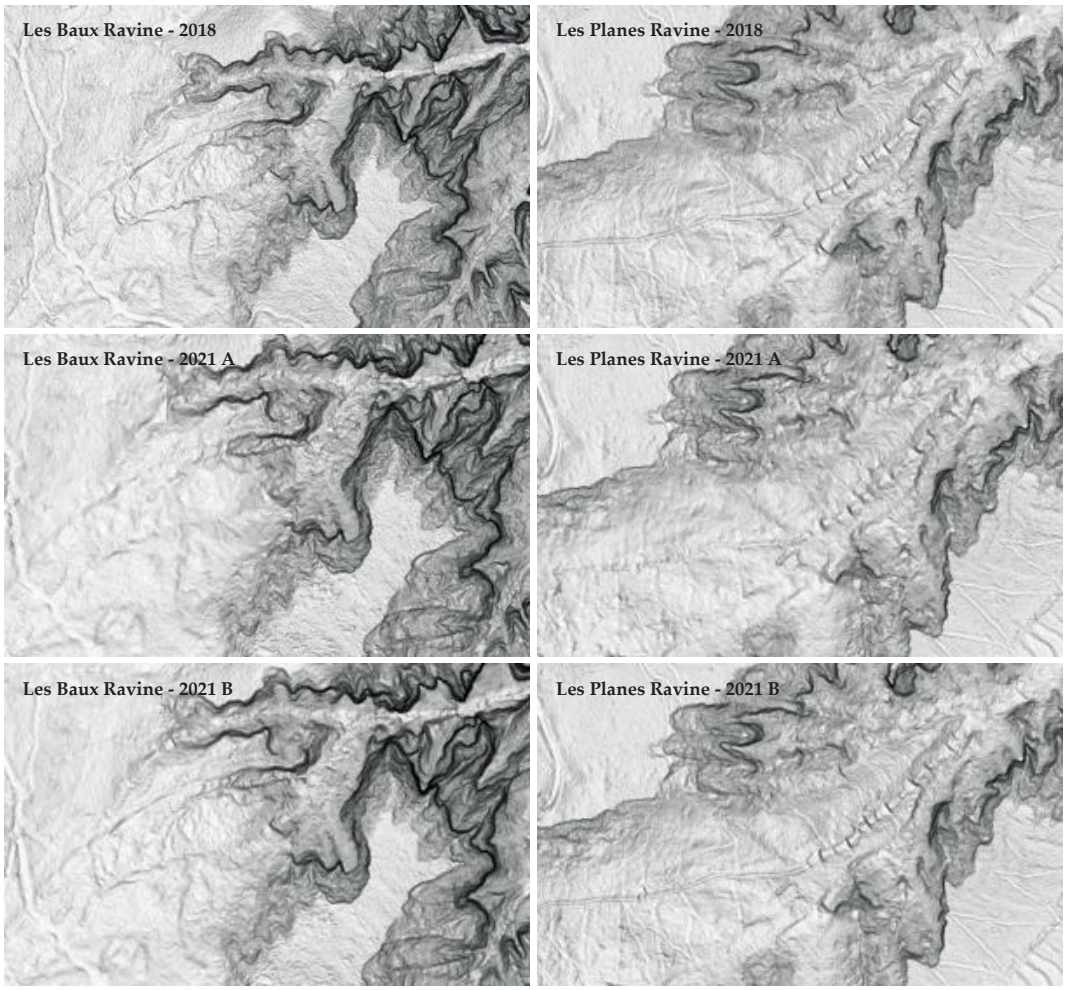

Figure 9: Examples showing areas of quality loss between flights.

The second processing step involves making the data available with specific formats and details. Most deliverables enable direct visualisation of data. Deliverables include a 1 m interval DTM in .asc format, a 10 cm MKP DTM in .xyz format, a 500 m by 500 m tile assembly table in .shp format, an orthophotograph in .ecw format, raw photographs in .jpg format. Some of the other deliverables correspond to quasi-raw data, i.e. the classified point cloud on 500 m tiles in .las format. These last files make it possible to reproduce processes and generate new data with different intervals.

When all the deliverables have been received, it becomes possible to carry out specific processing as input for the study. A distinction can be made between processing based on data from a single survey and processing that compares data from two surveys. Processing using data from a single LIDAR survey can have several purposes. Producing an exposure map with shading

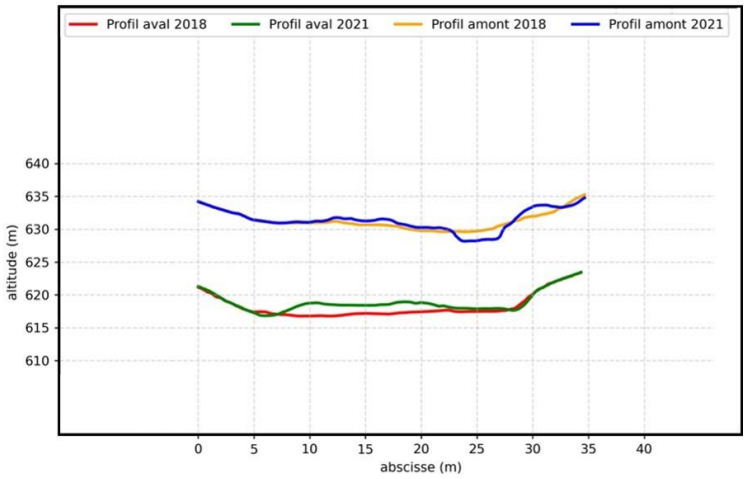

Figure 10: Examples of cross-section comparisons in the Baux Ravine

allows us to visualise the terrain on different scales. This perspective will be completed by a more detailed understanding of the topography through the production of slope maps playing with classes of values and associating isolines with different spacing. These items can provide a basis for mapping the geomorphology of the terrain studied. Finally, processing relating to the longitudinal and cross-sectional profiles of the watercourses will be useful in both the geomorphological and hydraulic parts of the study.

When two LIDAR surveys are available for the same study area, other processing steps may be considered, primarily to visualise and quantify changes to the terrain on several levels. In the first instance, visual comparisons could be made using orthophotographs and shading conducted on the two dates. The before and after views could be used to highlight receding areas on top of a bank or a scar indicating the start of a landslide. The second line of work involves quantifying the phenomenon of soil erosion and the accumulation of materials. Data can be processed on different scales, from the catchment area to a closely targeted area of just a few m^2, in order to quantify volumes of erosion and accretion *(Figure 11)*. This type of processing is particularly useful in cases where the terrain is predisposed to erosion following extreme rainfall events. Similarly and in addition, comparisons of longitudinal and cross-sectional profiles at various time intervals can highlight receding sections of the banks or even the elevation of a torrent bed at local level *(Figure 10)*.

This processing requires upstream pre-processing of the data, in order to make a comparison based on different time intervals. The comparison requires data that are "superimposable" in terms of location (point coordinates), scale (pixel resolution) and file format.

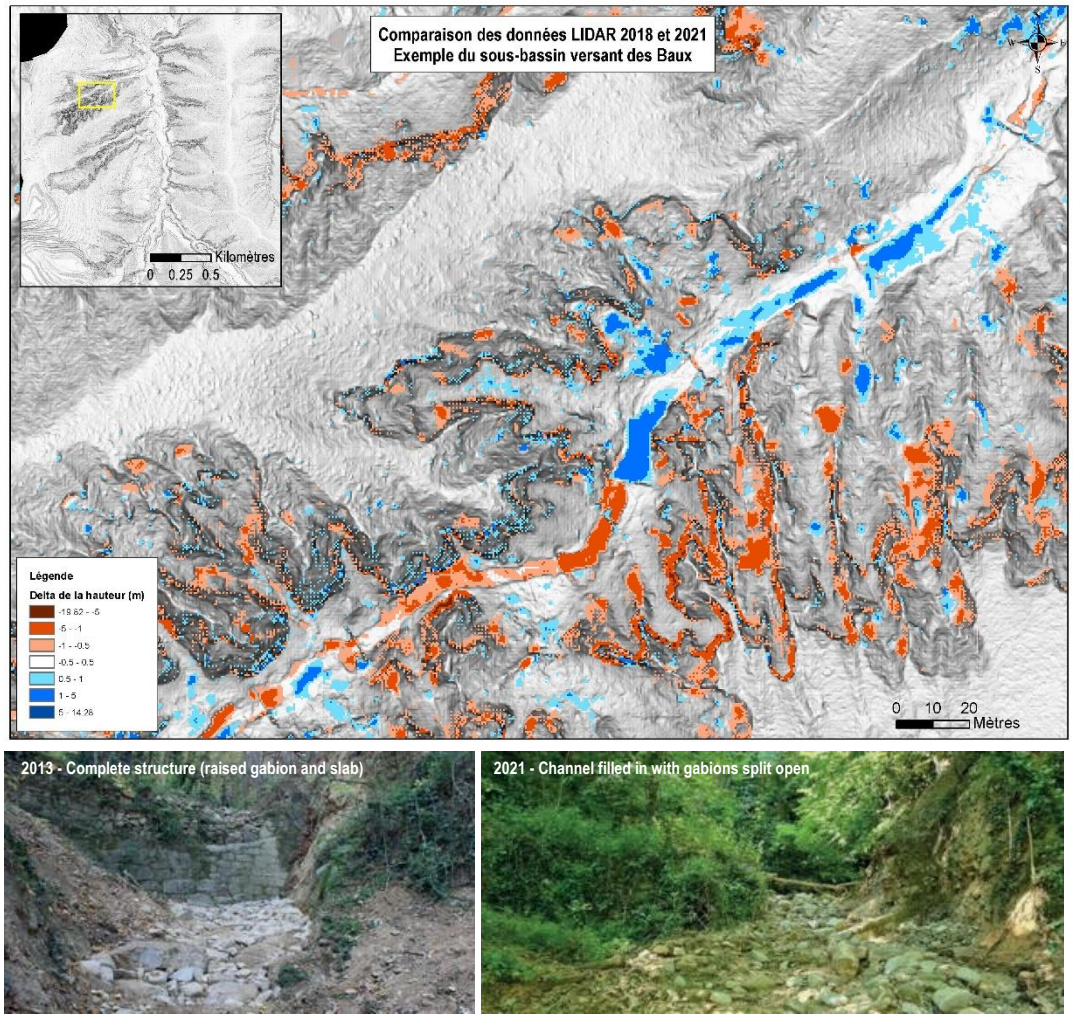

Figure 11: Comparison of LIDAR data 2018-2021 with an example of changes to structure B34 in the Baux Ravine.

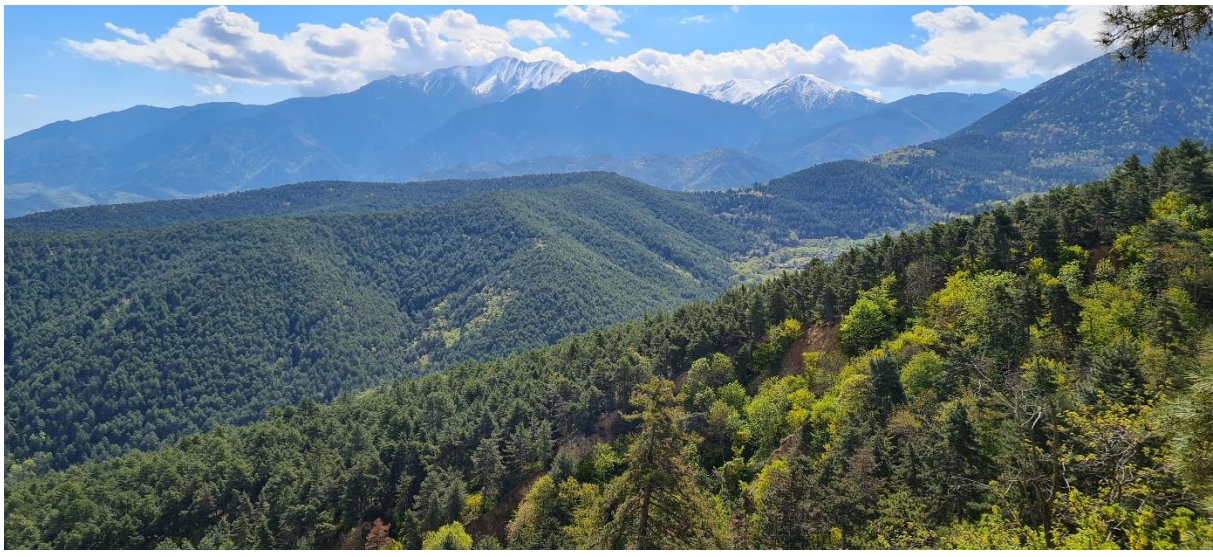

4. Analysis results

Simply processing the data is not enough to put the results into perspective. It is therefore necessary to analyse the data obtained and to view them critically, based on the nature and objectives of the survey launched. This is the approach developed below, following a comparison of LIDAR data from 2018 and 2021 with different resolutions.

All the values quoted below can be seen in *Figures 12 and 13.* The first processing step compared the data on a 0.50 m pixel grid, defined on an experimental, non-scientific basis, with the objective of assessing the volumes of eroded and accumulated materials in each sub-catchment area. The results were viewed critically, by targeting several areas and comparing them with the real terrain, using photographs. The spatial analysis highlighted a strong correspondence between the main upstream erosion zones and the downstream accumulation zones, particularly as the materials had not been picked up by the ravines in most cases, since there was no flood bed. However, at the same time, we observed isolated accumulation pixels, erosion zones without corresponding accumulation zones and vice versa. Questions were also raised concerning the vertical crest lines where the level of calculated erosion was over ten metres locally. Based on these initial observations, processing will be repeated with a grid of 1 m: the objective will be to assess changes to total volumes and by sub-catchment, as well as to answer any questions concerning the correspondence zones.

Processing the 1 m grid provided some of the answers to the questions above. Firstly, there was a significant decrease in total volumes, while the difference between them increased sharply: from -20% (-7,232.62 m²) between the eroded volume and the accumulated volume with the 0.50 m grid to 54% (-15,580.58 m²) with the 1 m grid. Secondly, differences were observed between the gullies on either side of the Baillmarsane: the differences between a precision level of 0.50 m and 1 m on the left bank were highly variable, while values on the right bank were more homogeneous. The phenomenon of isolated pixels was anecdotal and values appeared to be smoother, which could be explained by the larger grid. The comparison between the two processing operations highlights the advantages of processing data with several levels of precision in order to validate or invalidate trends resulting from spatial and statistical analysis. As a result, similar work on a finer 0.20 m grid is under way.

Cutting grid size to 0.20 m resulted in a significant de facto increase in overall volumes. Based on previous processing steps, the best overall balance was obtained with the 0.50 m grid size. However, at the level of each sub-catchment area, diverging trends reflected the personality of each gully highlighted above: some were balanced, others saw significant increases in accretion volumes. At the same time, the phenomenon of isolated accumulation pixels, already observed with the 0.50 m grid, was largely dominant here, primarily on the slopes of gullies on the left bank, and to a lesser extent on the right bank. The Clot de Lliby gully, the most anthropised sub-catchment area with the former Escaro mine, is the most significant example. Processing based on the 0.20 m grid nevertheless highlighted a specific point: if we start with a 1 m grid and descend to 0.20 m, erosion volumes increased per sub-catchment area with the greater level of precision, whereas accumulation volumes increased exponentially. It therefore seems that this processing step gives a different response for the erosion phenomenon and the accumulation phenomenon. Until now, the margin of error applied for the processing grid, i.e. -0.5 m/+0.5 m for a 0.5 m grid, was not taken into account in the calculations and was therefore considered as null. From this point, this cursor may be modified to partially extract isolated pixels without impacting erosion volumes that appear to be coherent.

The following results are therefore variations of processing steps with the 0.20 m grid, with changes to the positive value of the cursor applied to the margin of error. The first variation was therefore a 0.20 m grid with a margin of -0.2 m/+0.5 m. As a result, the accumulation volume fell significantly from 100,546.39 m² to 29,091.97 m². A comparison of the erosion and accumulation volumes by sub-catchment area shows that a positive margin of +0.5 m was too selective overall. The cursor will therefore be reduced to +0.4 m in the next processing step.

With a grid of 0.20 m and a margin of -0.2 m/+0.4 m, the total accumulation volume became more precise. The same was true at sub-catchment level. We can see that the volumes of the different gullies on the left bank started to balance out partially or even completely. On the right bank, the volumes started to even out, but the process remained less significant at this stage. We could therefore conduct a final processing step in which the cursor would be reduced to +0.3 m.

This last operation with a grid size of 0.20 m and a margin of -0.2 m/+0.3 m provided the best overall balance with a difference of just 4,611 m² between erosion and accretion volumes for Baillmarsane. However, for the gullies on the right bank and after a comparison with previous values, it seems that varying the cursor is not an effective response: a balance was observed in the gullies regardless of whether the grid size was 1 m or 0.20 m. Further, and in spite of a clear and constant improvement concerning isolated accumulation pixels, a number of them remained present on the slopes. Owing to their isolation, these pixels created a bias in statistics on accumulation volumes, particularly on the left bank. A final processing step will therefore be tested, based on geomorphological mapping of the sub-catchment area: the so-called active zones (in erosion, accumulation,

landslide and torrentiality) will be merged and combined with a 5 m buffer zone to include any overlooked upper slopes that may provide materials.

Trimming the sub-catchment areas with a 0.20 m grid to include only active areas did not give significant results. While differences tended to decrease, the balance was less favourable than in previous processing steps. Looking at all these processing operations, it is easy to see that there is no single, homogeneous processing step to correctly match up erosion and accumulation. Moreover, each processing step includes a number of biases, to which we may add those relating to acquisition, pre- and post-processing and spatial and statistical data analyses.

ESTIMATION DES VOLUMES ERODES ET ACCUMULES - MAILLE 1m

	NOM	VOL. EROSION	VOL. ACCUMULATION	DIFFERENCE	
	Total (m3)	28910.11	13329.53	-15580.58	-54%
RIVE GAUCHE	Source	1934.42	747.77	-1186.65	-61%
	Baux	11940.00	4933.34	-7006.66	-59%
	Sola des Pierres	2266.53	1324.36	-942.17	-42%
	Baux des Planes	4727.01	2625.54	-2101.47	-44%
	Clot de Lliby	4913.71	2361.05	-2552.66	-52%
RIVE DROITE	Campreste	213.05	265.92	52.87	25%
	Mangré	1102.40	284.29	-818.11	-74%
	Coma del Mas	662.05	229.27	-432.78	-65%
	Coste	552.50	205.45	-347.05	-63%
	Fourche	415.90	254.10	-161.80	-39%
	Vignes	182.54	98.44	-84.10	-46%

ESTIMATION DES VOLUMES ERODES ET ACCUMULES - MAILLE 0.50m

	NOM	VOL. EROSION	VOL. ACCUMULATION	DIFFERENCE	
	Total (m3)	36636.77	29404.15	-7232.62	-20%
RIVE GAUCHE	Source	2445.68	2113.76	-331.92	-14%
	Baux	16039.30	6718.65	-9320.65	-58%
	Sola des Pierres	2857.33	2964.20	106.88	4%
	Baux des Planes	5510.55	7123.25	1612.70	29%
	Clot de Lliby	4371.80	8895.80	4524.00	103%
RIVE DROITE	Campreste	541.05	309.96	-231.09	-43%
	Mangré	1366.20	399.98	-966.22	-71%
	Coma del Mas	1570.83	346.51	-1224.32	-78%
	Coste	985.93	210.95	-774.99	-79%
	Fourche	687.65	200.30	-487.36	-71%
	Vignes	260.46	120.81	-139.66	-54%

ESTIMATION DES VOLUMES ERODES ET ACCUMULES - Maille 0.20 m

	NOM	VOL. EROSION	VOL. ACCUMULATION	DIFFERENCE	
	Total (m3)	51333.08	100546.39	49213.31	96%
RIVE GAUCHE	Source	3540.63	5518.56	1977.93	56%
	Baux	19883.40	14341.80	-5541.60	-28%
	Sola des Pierres	3734.75	8536.56	4801.81	129%
	Baux des Planes	7734.28	18123.92	10389.64	134%
	Clot de Lliby	8263.16	45268.40	37005.24	448%
RIVE DROITE	Campreste	1018.55	1877.68	859.14	84%
	Mangré	2008.08	1670.36	-337.72	-17%
	Coma del Mas	2058.29	1235.24	-823.04	-40%
	Coste	1484.86	1306.32	-178.54	-12%
	Fourche	1073.74	1386.02	312.28	29%
	Vignes	533.34	1281.52	748.18	140%

ESTIMATION DES VOLUMES ERODES ET ACCUMULES - MAILLE 0.20 m -0.2/+0.5m

	NOM	VOL. EROSION	VOL. ACCUMULATION	DIFFERENCE	
	Total (m3)	51333.08	29091.97	-22241.11	-43%
RIVE GAUCHE	Source	3540.63	1981.17	-1559.46	-44%
	Baux	19883.40	6737.44	-13145.96	-66%
	Sola des Pierres	3734.75	2891.39	-843.36	-23%
	Baux des Planes	7734.28	6875.76	-858.52	-11%
	Clot de Lliby	8263.16	8921.24	658.08	8%
RIVE DROITE	Campreste	1018.55	345.71	-672.84	-66%
	Mangré	2008.08	397.42	-1610.66	-80%
	Coma del Mas	2058.29	361.95	-1696.34	-82%
	Coste	1484.86	225.17	-1259.68	-85%
	Fourche	1073.74	228.40	-845.35	-79%
	Vignes	533.34	126.31	-407.03	-76%

ESTIMATION DES VOLUMES ERODES ET ACCUMULES - MAILLE 0.20 m -0.2/+0.3m

	NOM	VOL. EROSION	VOL. ACCUMULATION	DIFFERENCE	
	Total (m3)	51333.08	55944.78	4611.70	9%
RIVE GAUCHE	Source	3540.63	3577.66	37.03	1%
	Baux	19883.40	10419.32	-9464.08	-48%
	Sola des Pierres	3734.75	5098.72	1363.97	37%
	Baux des Planes	7734.28	11890.20	4155.92	54%
	Clot de Lliby	8263.16	21013.44	12750.28	154%
RIVE DROITE	Campreste	1018.55	832.40	-186.14	-18%
	Mangré	2008.1	819.55	-1188.53	-59%
	Coma del Mas	2058.29	753.47	-1304.82	-63%
	Coste	1484.86	550.86	-934.00	-63%
	Fourche	1073.74	605.52	-468.22	-44%
	Vignes	533.34	383.64	-149.70	-28%

ESTIMATION DES VOLUMES ERODES ET ACCUMULES - MAILLE 0.20 m -0.2/+0.4m

	NOM	VOL. EROSION	VOL. ACCUMULATION	DIFFERENCE	
	Total (m3)	51333.08	38898.28	-12434.80	-24%
RIVE GAUCHE	Source	3540.63	2633.51	-907.12	-26%
	Baux	19883.40	8320.08	-11563.32	-58%
	Sola des Pierres	3734.75	3723.23	-11.52	0%
	Baux des Planes	7734.28	8929.36	1195.08	15%
	Clot de Lliby	8263.16	12818.60	4555.44	55%
RIVE DROITE	Campreste	1018.55	512.32	-506.23	-50%
	Mangré	2008.1	548.07	-1460.01	-73%
	Coma del Mas	2058.29	517.67	-1540.62	-75%
	Coste	1484.86	332.31	-1152.54	-78%
	Fourche	1073.74	360.57	-713.18	-66%
	Vignes	533.34	202.55	-330.79	-62%

Figure 12: Tables of estimated eroded and accumulated volumes with various grid sizes.

RESULTATS PROBANTS DES DIVERS TRAITEMENTS

	NOM	VOL. EROSION	VOL. ACCUMULATION	DIFFERENCE		TRAITEMENT
	Total (m3)	51333.08	55944.78	4611.70	9%	Maille 0.20m -0.2m/+0.3m
RIVE GAUCHE	Source	3540.63	3577.66	37.03	1%	Maille 0.20m -0.2m/+0.3m
	Baux	19883.40	14341.80	-5541.60	-28%	Maille 0.20m
	Sola des Pierres	3734.75	3723.23	-11.52	0%	Maille 0.20m -0.2m/+0.4m
	Baux des Planes	7734.28	6875.76	-858.52	-11%	Maille 0.20m -0.2m/+0.5m
	Clot de Lliby	8263.16	8921.24	658.08	8%	Maille 0.20m -0.2m/+0.5m
RIVE DROITE	Campreste	213.05	265.92	52.87	25%	Maille 1m
	Mangré	2008.08	1670.36	-337.72	-17%	Maille 0.20m
	Coma del Mas	662.05	229.27	-432.78	-65%	Maille 1m
	Coste	1484.86	1306.32	-178.54	-12%	Maille 0.20m
	Fourche	415.90	254.10	-161.80	-39%	Maille 1m
	Vignes	182.54	98.44	-84.10	-46%	Maille 1m

Figure 13: Table showing the conclusive results of the various processing steps.

5. Limitations on the use of LIDAR data

From the acquisition of data through to their exploitation, many biases need to be taken into account in the use and analysis of data. Many parameters come into play in these various phases. These parameters are associated with biases, i.e. limits that are open to question and that can throw into doubt the relevance of using or analysing the data.

In the data acquisition phase, biases are linked to the order, the techniques and tools used and the conditions of acquisition. For example, it is useful to involve the same service provider in acquisition at different dates in order to obtain the most homogeneous data. They will be more likely to use the same equipment and apply the same settings from one acquisition to another. The last survey gave the RTM department the hindsight necessary to adapt the specifications in order to better take account of previous LIDAR acquisition(s) and to establish the first survey as a reference. Finally, biases independent of the provider play an important role and should not be overlooked: the acquisition period (the season or even the month) and the flight conditions (visibility, wind). For example, we were able to observe the impact of vegetation cover between three acquisitions: the period of April 2018 corresponded to a period of vegetative rest where the leaves and shrubbery were in the early stages of development, making it possible to obtain a sufficient quantity of ground points; in June 2021, the vegetation was luxuriant, making it difficult for the lasers to penetrate and resulting in uncertain or even incomplete terrain modelling in places; in November 2021, the vegetation was less dense again, as in April 2018. In addition, even if conditions are optimal and the tools identical, reproducing reality with a model can never give a totally compliant result. The margin of error created in the acquisition phase will, moreover, be supplemented by other subsequent margins of error at a later stage. It is therefore necessary to be aware of these margins of error and to take them into consideration through to the end of the study.

The processing phase, which includes both pre-processing by the service provider and post-processing by the study authors, also generates a number of biases. In pre-processing, the main biases stem from the algorithms used in point classification.

Classification errors can cause significant deviations in terrain modelling: the classification of vegetation as ground points and vice versa will locally modify the topography representing the real situation. We experienced this in an area close to a house. Between 2018 and 2021, an area was cleared of all shrubbery. In April 2018, the points acquired were classified as ground points, despite the presence of dense shrubbery that could not be penetrated by the rays; in 2021 the vegetation was removed and the points obtained were classified as ground points. When comparing LIDAR data, an area of erosion appeared in the vegetation cover in 2018: this is an artifact since it was not an erosion of materials but an "erosion of vegetation" caused by a misclassification of the original points. This deviation was also visible according to the orientation of certain gullies: locally, an accumulation could be seen on the north-facing banks where the presence of vegetation is far greater than on the south-facing banks. It is therefore possible that this extensive vegetation interfered with the November 2021 survey, compared with the 2018 survey.

Finally, biases may be associated with the level of precision applied when comparing LIDAR data, for example. The comparison studies previously developed and carried out at several levels of precision (1 m, 0.5 m and 0.2 m) produced highly variable results, not only from one level of precision to another, but also from one bank to another. This significant deviation is the result of several factors: the extent of damage to a gully following Storm Gloria, the persistence of vegetation, the orientation of the banks, the proportion of very steep banks, the proportion of anthropised terrain that can modify the topography locally. It therefore seems necessary to work on several different scales and with several levels of precision to define the most coherent cause-effect correlations.

One final category of bias refers to spatial and statistical analyses. The data produced must be analysed according to the questions addressed and on a scale appropriate to the phenomena. This was what we did after processing with the 20 cm grid: the left bank of the Baillmarsane was strongly impacted by isolated accumulation pixels, which significantly increased volumes. Specific processing steps were applied, such as varying the margin of error cursor or focusing only on the so-called active areas identified through geomorphology, in order to establish a possible balance between erosion and accumulation volumes. We saw that this work did not provide a significant response for the gullies on the right bank of the Baillmarsane, where Storm Gloria had little impact.

It is therefore necessary to take a critical look at the various analyses reflecting divergent trends, especially as the interpretation of data, particularly statistical data, remains subjective.

Interreg Sudoe
EUROPEAN UNION
MONTCLIMA
European Regional Development Fund

www.montclima.eu